Adsorption (2008) 14: 189–199
DOI 10.1007/s10450-007-9069-6

Modelling of patterns during adsorption of chiral molecules on metallic surfaces

R.O. Uñac · A.M. Vidales · M.V. Gargiulo · J.L. Sales · G. Zgrablich

Received: 27 April 2007 / Revised: 2 October 2007 / Accepted: 8 October 2007 / Published online: 4 December 2007

Abstract A gas lattice model and Monte Carlo simulations have been used to model the behavior of chiral molecules adsorbed on clean metallic surfaces. The aim of this work is to characterize how adsorbed molecules organize on the surface, what their footprints are and which are the main mechanisms of interaction responsible for the different patterns observed. These patterns have already been depicted and illustrated by other authors through different techniques and here some of them have been simulated using simple models for adsorption. In these models, both inhibition effects (such as blockage of neighboring sites to simulate steric effects) and promotion of neighboring sites (to simulate adsorbate-adsorbate and adsorbate-substrate interactions) are used. These adsorption rules try to mimic the enantiomeric character of the adsorbed species.

Keywords Chiral · Enantiomer · Adsorption

1 Introduction

Over the last decade much research has been done on the subject of adsorption of chiral organic molecules onto metallic surfaces. These organic-metal systems have captured special attention of scientists because of their important applications mainly in the pharmaceutical and technological fields (Williams et al. 1996; Barlow and Raval 2003; Humblot et al. 2004; Humblot and Raval 2005; Romá et al. 2004). This interest is assisted and encouraged by the great improvement in experimental microscopic and spectroscopic techniques, such as, reflection absorption infrared spectroscopy (RAIRS), X-ray photoelectron spectroscopy (XPS), low energy electron diffraction (LEED) and scanning tunneling microscopy (STM), conforming a set of multi-technique approach to study the supra-molecular adsorption structures in the above systems. All this sums up to the great advances in simulation techniques and numerical ab initio packages that allow to resolve, at least partially, the problem of adsorption not only of simple molecules but also of more complex systems as those arising from the organic-metal interfaces.

Under appropriate conditions, the adsorption of an enantiomerically pure chiral species may lead to the formation of patterns that are chiral themselves, thus generating an "extended chirality" (Barlow and Raval 2003; Humblot et al. 2004; Humblot and Raval 2005). The scale of these chiral patterns ranges from nano-structures of few molecules to macroscopic dimensions (Williams et al. 1996; Stensgaard 2003). It is known that the nature of these bi-dimensional patterns depends on the balance among adsorbate-substrate and adsorbate-adsorbate interactions (Ranking and Sholl 2004, 2005). However, some general characteristics seem to emerge for many of these structures (Stensgaard 2003): (a) chiral molecules adsorb in different configurations (or "adsorbed species"), like, for example, flat, tilted, dimer-like or monomer-like, depending on the coverage; (b) the structures themselves change with surface coverage and may preserve or not the extended chirality feature; (c) interactions leading to extended chirality must be strongly non-isotropic.

R.O. Uñac (✉) · A.M. Vidales · G. Zgrablich
Laboratorio de Ciencia de Superficies y Medios Porosos, Departamento de Fisica, Universidad Nacional de San Luis and CONICET, Ejército de los Andes 950, 5700 San Luis, Argentina
e-mail: runiac@unsl.edu.ar

M.V. Gargiulo · J.L. Sales
Departamento de Física and Instituto de Energía Eléctrica (CONICET), Universidad Nacional de San Juan, Av. Libertador 1100 Oeste, 5400 San Juan, Argentina

A great deal of work has been done in order to understand this behavior and some of the main papers that attracted our attention for the present work are those by Chen et al. (2002), Toomes et al. (2003) and Barlow et al. (1998, 2005). The former studied the system glycine on Cu(110) and observed, using high resolution STM techniques, induced surface chirality showing two domains with different internal molecular arrangements: a homochiral domain presenting a pseudo-centered structure and a heterochiral domain with a clear glide plane symmetry. Since the diffraction pattern from the homochiral pseudo-centered structure is part of the diffraction pattern of the heterochiral structure, the overall diffraction pattern that they obtain will show glide plane symmetry. The existence of two possible domains for the adsorption of glycinate on Cu(110) is in coincidence with the work of Barlow et al. (1998).

On the other hand, Toomes et al. conclude in their work that there is actually no compelling evidence for the existence of homochiral domains on either Cu(110) and Cu(100) surfaces. They say that the only specific evidence in favor of this interpretation is differences in STM images which they think could be attributed to the presence of artifacts of the experimental technique.

Finally, authors in Refs. (Barlow et al. 2004, 2005) study the polymorphism in supramolecular chiral structures of R- and S-alanine on Cu(110). With the help of different experimental techniques, they determine the local and supramolecular adsorption structures created by the enantiomeric forms of alanine molecules adsorbed on that metallic surface. The organization and chirality of the observed structures are discussed on the basis of the two aspects of the problem: inherent molecular chirality and footprint chirality of the alaninate. In their work, different hypothesis have been advanced in order to explain the observed polymorphism, also suggesting a model to explain their observations (Barlow et al. 2004, 2005).

Based on the above evidence, our purpose here is to discuss, in the context of very simple simulation models for adsorption, the molecule-surface characteristics (geometric and energetic) which could give rise to the formation of bidimensional organization of adsorbed species, being this adsorbed molecules chiral or non-chiral in their gas phase. Besides, molecules may transfer their chiral character to the surface of the substrate through the so called molecular footprint. This model can be also easily applied to the adsorption of a racemic mixture, as it will be shown below.

The following section deals with the simulation model details and the main definitions needed to understand our model. Next, we present and discuss our results and, finally, we outline our conclusions.

2 Modelling of chiral molecules adsorbing on a metallic surface

To simulate adsorption, we basically use a lattice-gas model and a Monte Carlo technique. The metallic surface is represented by a square lattice of equivalent adsorption sites. To simplify the model, we will not take into account the chirality of molecules in their gas phase, i.e., before adsorption occurs. As a result of adsorption, a molecule will cause the occupation of a set of sites on the network and will also modify their neighbors, thus defining what we will call a "footprint" of the chiral molecule on the metallic surface. In simulations, we keep adsorbing until almost saturation.

Several different footprints could be chosen in this scenario, but we only selected the ones that better represent the adsorption characteristics of chiral molecules like S- and R-alanine or even the simplest case of glycine (Barlow et al. 2005). Among those, we used two different models that we name "A" and "B", respectively.

In Fig. 1 we depict schematically the footprints generated by an adsorbed molecule in the context of model A. Each enantiomer (suppose S-alanine) may adsorb as two different species named α_3 (with two possibilities: ◹ and ◿) and α_2 (with three possibilities: |, \ and /), giving place to the geometrical shapes drawn in parts (a), (b) and (c).

To mimic the (unknown) adsorbate-substrate and adsorbate-adsorbate interactions, we use a promotion mechanism during the adsorption of new molecules from the gas phase to simulate the interactions that change the energy topography of the surface, favoring the adsorption of new molecules (gray sites in Fig. 1). In addition, the steric effect of exclusion due to the chiral structure of the molecule is taken into account by the inhibition of particular nearest neighbor sites for the adsorption of molecules in the neighborhood of an already adsorbed one. In summary, an adsorbed chiral molecule is represented by an array of chemical groups of three (two) sites for $\alpha_3(\alpha_2)$ with a chiral center C (indicated with an arrow in Fig. 1) and neighboring sites (signed as N in that same figure) thus defining the possible molecular footprints. The site of the metallic surface taken as the center is completely occupied by the molecule and cannot be shared with any other and defines the neighborhood of the molecule. The other two (one) N-sites of the surface can be shared by another molecule only as N sites. In this way, when a molecule is adsorbed on the surface two interactions can occur: inhibitions due to steric effects and promotion of neighboring sites. The new molecules can only adsorb on promoted sites and this requires that seeds or defects have to be set initially. Irreversible adsorption is considered and diffusive effects are not taken into account. Model A may fairly represent the proposed models for adsorption of glycinate and alaninate on Cu(110) discussed in Barlow et al. (2005).

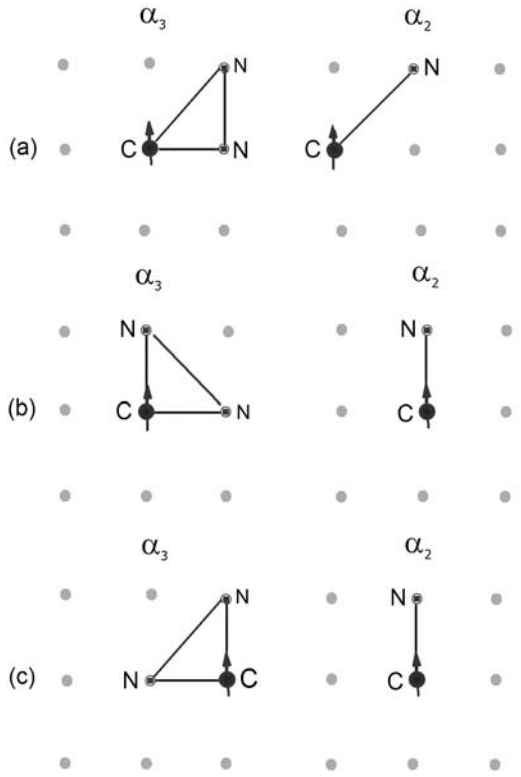

Fig. 1 Schematic representation of the footprints in model A for adsorbed molecules on the square lattice. Different kinds of sites are indicated: *C*, chiral center site; *N*, neighboring sites; *gray solid circles* represent promoted sites. (**a**) Corresponds to footprints used in case 1. (**b**) Corresponds to footprints used in case 2. (**c**) Corresponds to footprints used in case 4

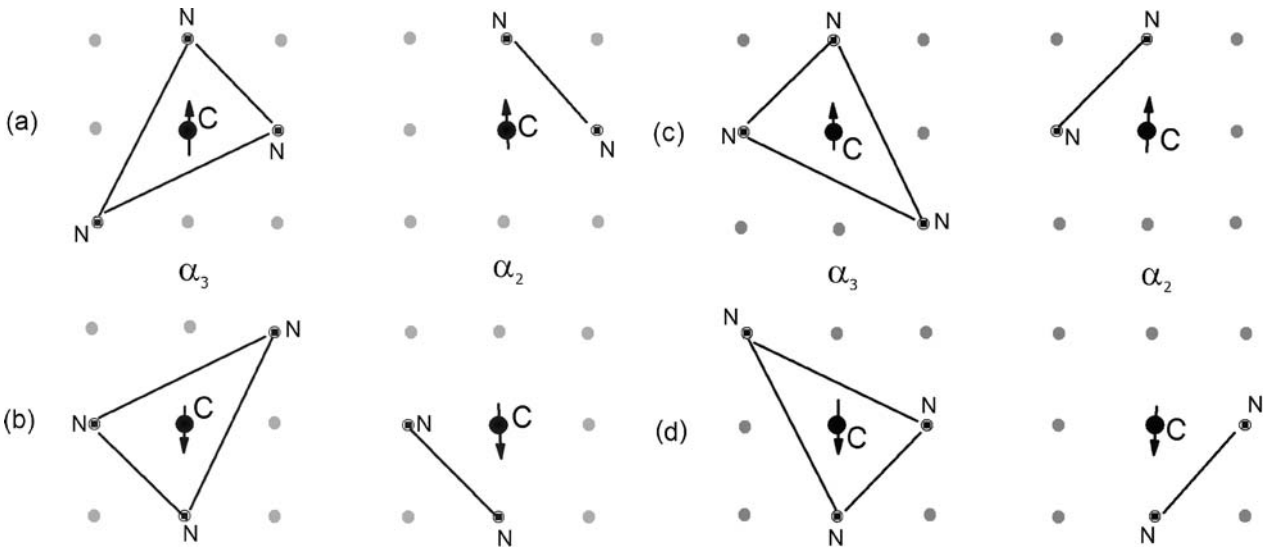

Fig. 2 Schematic representation of the footprints in model B for adsorbed molecules on the square lattice. Different kinds of sites are indicated: *C*, chiral center site; *N*, neighboring sites; *gray solid circles* represent promoted sites. (**a**) Corresponds to non rotated species of S-molecules. (**b**) Corresponds to rotated species of S-molecules. (**c**) Corresponds to non rotated species of R-molecules. (**d**) Corresponds to rotated species of R-molecules

In Fig. 2, we depict the footprint used in model B. Here, for a given enantiomer (R or S) two possibilities are also considered, named α_3 and α_2, as shown in Figs. 2a, 2c. The chiral center is indicated with an arrow. The molecule can be thought of as adsorbed on a four (three) sites structure on the surface: its center (C) and three (two) neighboring sites (N) for α_3 (α_2), defining the footprint of the molecule. As in model A, the site of the metallic surface taken as the center is completely occupied by the molecule and cannot be shared with any other. The other three (two) N-sites of the surface can be shared by another molecule only as N sites.

In model B we allow two possible rotations for α_3 footprint: "simple" rotations (SR), as shown in Figs. 2b, 2d on the left, and "complex" rotations (CR), as shown in Figs. 2b, 2d on the right.

Concerning adsorption, different kinds of mechanisms are possible for both models. A sequential process, in which, once a site on the surface has been randomly selected, we always try to adsorb a α_3 footprint. If this is not possible, we try to adsorb it with another footprint, trying again until a particular sequence is completed, as will be indicated further on. The other mechanism is a random process, in which we choose randomly, with the same probability among α_3 species. If this is not possible, we try to adsorb α_2 species. In both mechanisms, once a molecule is adsorbed, sites C and N are labeled.

If promotion of sites is implemented, the rest of the empty neighboring sites are set as promoted (gray sites on Figs. 1 and 2) and the center of new molecules from the gas phase can only adsorb on these promoted sites. Otherwise, if no promotion is implemented, the center (C) of new molecules can adsorb on empty sites, anywhere.

The order of the species in the sequences above and the promotion of sites, represents (in some qualitatively way) the different relative intensity of the adsorbate-substrate and adsorbate-adsorbate interactions for each species.

3 Results and discussion

3.1 Pure enantiomer adsorption

3.1.1 Model A

As explained above, in this model we use the footprints depicted in Fig. 1. We did simulations adsorbing only one type of enantiomer and we present different possibilities among the motifs shown in Fig. 1, inspired in the cases proposed by Barlow et al. (2005).

Case 1. In this case and in the following ones below, we use a sequential adsorption routine with promotion of neighboring sites. The present case has the following steps. First we randomly set a given number of seeds of α_3 molecules on the surface. Then, we choose randomly an adsorption site and try to adsorb a α_3 species. If this can not be done, we try to adsorb a α_2. The footprints used in this case are those shown in Fig. 1a. The results are shown in Figs. 3a and 3d. The upper part of the figure is a snapshot of the adsorbed molecules on the substrate. The lower part presents the behavior of the coverage for each species against the total coverage of the surface until saturation. Double chains of molecules $\alpha_3\alpha_2$ are developed. The molecules start to nucleate at the neighborhood of the seeds and grow into very large and twin chain structures. There is a markedly tilted alienation of the chains. No compact phases appear and the coverage of each species grows almost linearly, species α_3 being the most adsorbed, see Fig. 3d. The observed behavior is explained because of the steric effects introduced in the model related to the shape of the footprints and also to the adsorbate-substrate and adsorbate-adsorbate interactions given through the promotion and inhibitions of neighboring sites.

Case 2. We use the same protocol as in the precedent case but now the footprints are those depicted in Fig. 1b. Results are shown in Figs. 3b and 3e. Simple chains of α_3 species are developed and they organize in compact phases. These chains are most of the time interrupted by the adsorption of α_2 species. This pattern is again due to the interplay between steric effects and interactions. In this case the α_3 footprint used is better assembled on the surface, growing in an ordered array oriented in a tilted preferential direction. The evolution of coverage is linear and adsorption of α_2 specie is low.

Case 3. It is just a statistical mixture of cases 1 and 2. With a given likelihood for each case, we choose randomly which set of footprints we will try to adsorb sequentially among those shown in Figs. 1a or 1b. Results are in Figs. 3c and 3f. The pattern of adsorption shows the presence of domains of α_3 species with footprint corresponding to case 2. They are arranged in single chain ensembles (like those in case 2) competing with double chains of $\alpha_3\alpha_2$ pairs. Short vertical chains of α_3 footprint belonging to case 1 are observed. At high coverage, the likelihood for adsorption of α_2 tilted footprint (Fig. 1a) increase at the expense of α_3.

Case 4. This case corresponds to the footprints in Fig. 1c. The order in the adsorption sequence coincides with the order shown in the same figure. In the results illustrated in Fig. 4, we observe the same single chains of α_3 as in case 2 and we also find isolated short double chains of pairs α_2-α_2 in a practically perpendicular direction respect to the one followed by α_3 chains. These short chains stop the growth of the single chains. The presence of the tilted α_2 motif is crucial for the appearance of two different orientations on the surface. This shows up clearly when comparing Figs. 3b and 4a. As usual, we show the coverage evolution in Fig. 4b.

Case 5. When a molecule is going to be adsorbed, we select at random (with a given probability) among the two possible footprints α_3 (Figs. 1a and 1b, left). As pointed out above, this procedure reproduces the proposed chiral adsorption motifs for molecules like glycinate and alaninate over Cu(110) (Barlow et al. 2005). In the case of glycinate, the two motifs are equally likely and in the case of alaninate, they are slightly different. Here we will consider them

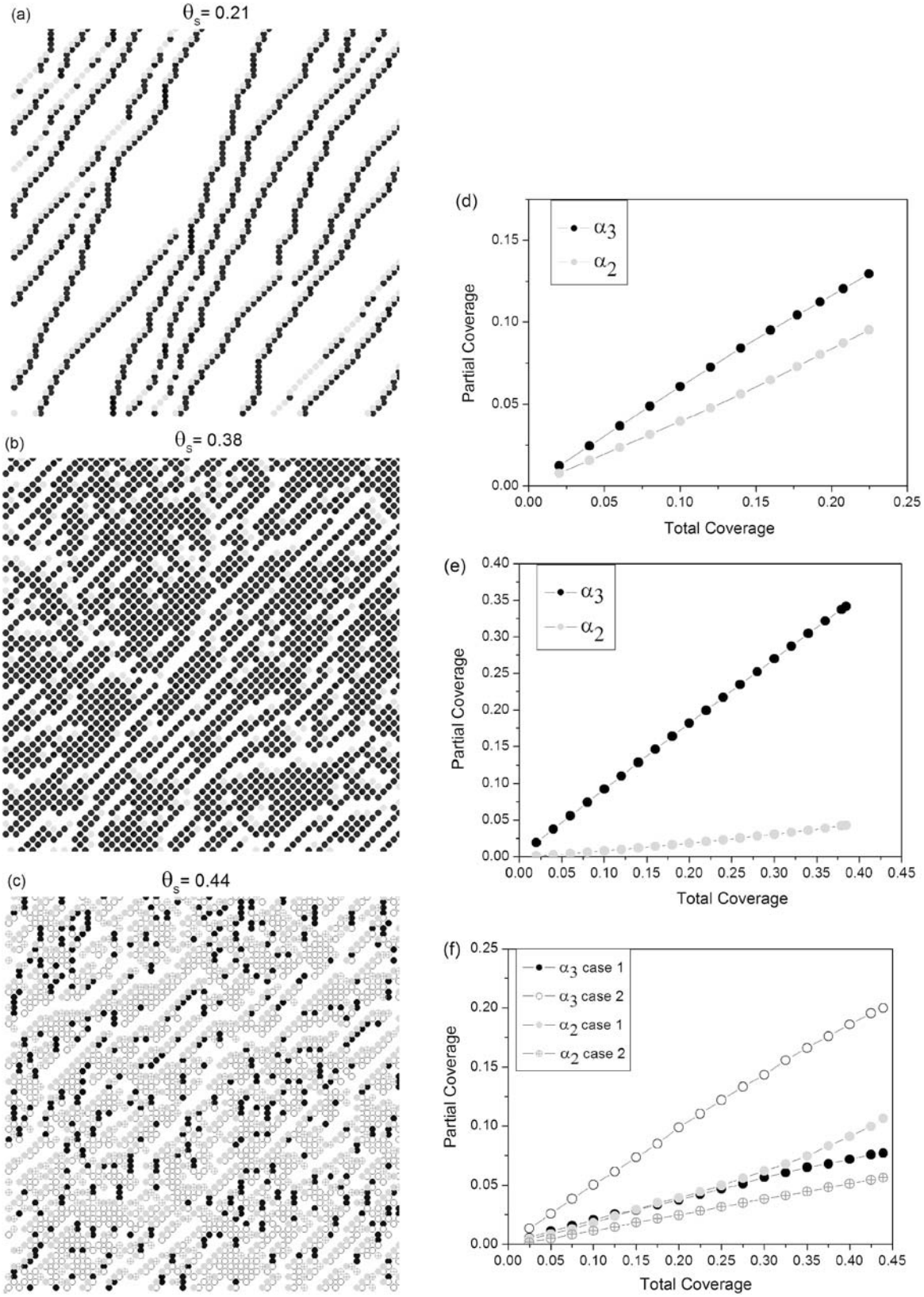

Fig. 3 Snapshots of surfaces belonging to different cases of model A. (**a**) Case 1, using footprints depicted in Fig. 1a. (**b**) Case 2, using footprints shown in Fig. 1b. (**c**) Statistical mixture of cases 1 and 2; the probability of choosing either case is 30%–70%, for cases 1 and 2, respectively. Parts (**d**), (**e**) and (**f**) show the coverage for each species against total coverage, respectively. Symbols are indicated in the *insets* of those last figures

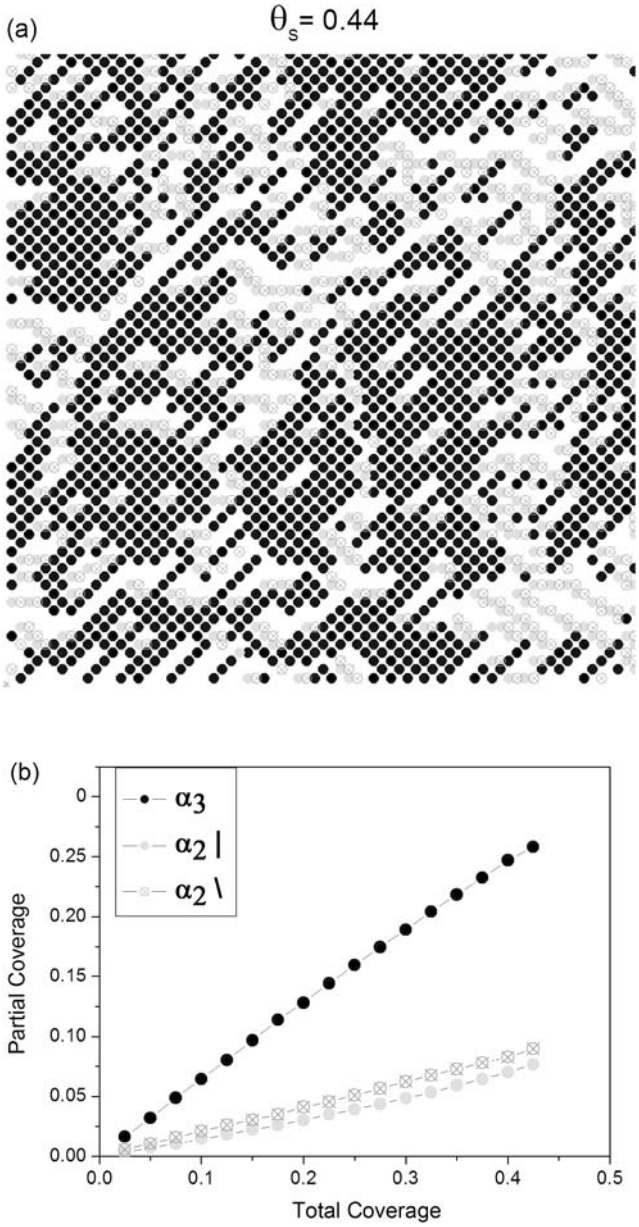

Fig. 4 (**a**) Snapshot of a surface corresponding to case 4, using footprints indicated in Fig. 1c. The order in the adsorption sequence coincides with the order shown in that figure. (**b**) Corresponding coverage evolution as a function of total coverage

equally probable in both cases. In Fig. 5 we present results for two cases. Part (a) shows the pattern where adsorption of α_3 molecules promotes the neighboring sites in the same way, no matters which motif is being adsorbed. The behavior observed in the figure resembles the one found for the adsorption of glycinate over Cu(110) in Chen et al. (2002). On the other hand, Fig. 5b shows the pattern where adsorption of α_3 molecules promotes the neighboring sites in a different way depending on which motif is being selected, thus favoring the adsorption of the same kind of molecules in the neighborhood. In this way we try to mimic the presence of the chemical groups that cause the two motifs to be energetically different (Barlow et al. 2005). As can be observed, two condensed phases are formed. Inside each phase, we find molecules with only one type of adsorption motif. They form single chains with two different preferential directions, one for each phase. This last result has not been observed experimentally to our knowledge. Evolution of partial coverage as a function of total coverage is illustrated in parts (c) and (d) on the same figure. As observed in part (d), there is a non linear behavior in the partial coverage. This demonstrates a competition between species due to the fact that promotion here is different for each adsorbing species.

Within the framework of this simple model and according to the experiments in Barlow et al. (2005) and to the above results, we may state that a chiral molecule, like for instance alanine, transfers its chiral character to its footprint as a unique motif (with a given and definite orientation in the surface) in such a way that a molecule with a given chirality can not give rise to different chiral footprints. Otherwise, in experiments it would be found the existence of chains following more than one overall growth direction.

3.1.2 Model B

Based on the results obtained with model A, we extend our analysis to a more complex representation of the chiral structure of the simulated molecules, taking into account, for instance, the rotational degree of freedom of the motifs.

In the context of this model, our results indicate that the features and direction of the patterns formed on the surface depend not only on the molecular structure but also on the way in which it interacts with the surface and with the other already adsorbed molecules. Basically, we can classify the obtained patterns into two groups, depending on the extent of the single and double chiral chain assemblies that they show. In all the cases studied, the chains are orientated in a distinct preferred chiral growth direction and orientation on the surface. This direction is the same as the one of the chiral structural axis of the molecule. In what follows in this section we present results for the case of S-molecules, Figs. 2a and 2b.

Short range order In this group we observe the development of short double and single chains of molecules, randomly distributed on the substrate. The adsorption mechanism employed here does not give rise to nucleation and growth because we do not use seeds or defect, and neither can the adsorbed molecule promote any adsorption of a new molecule next to it. Nevertheless, we observe simple and double short chains due to steric effects related to the accommodation of adsorbed molecules, building up a dispersed phase.

Figure 6 shows examples of this group. The upper part of the figure shows snapshots of the adsorbed molecules on the

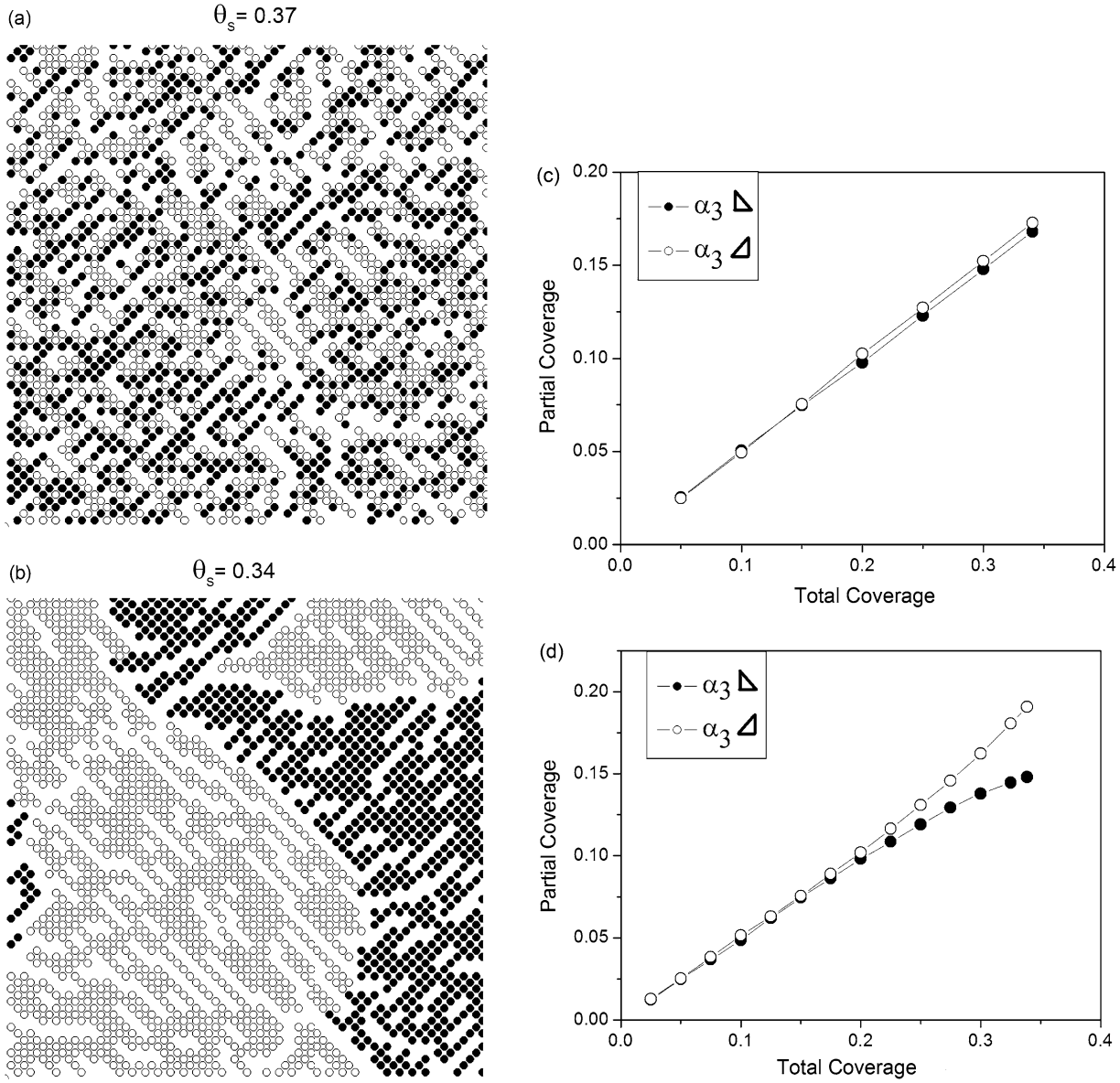

Fig. 5 Snapshots of surfaces corresponding to case 5, using footprints α_3 depicted in Figs. 1a and 1b, left. (**a**) Pattern where adsorption of α_3 molecules promotes the neighboring sites in the same way. (**b**) Pattern where adsorption of α_3 molecules promotes the neighboring sites in a different way. (**c**) Linear behavior of partial coverage corresponding to part (**a**); no competition among species is present. (**d**) Non linear behavior of coverage corresponding to the snapshot in part (**b**), showing a competition among species. *Triangles* help to identify the footprints used in this case

substrate. The lower part presents the behavior of the coverage for each species against the total coverage of the surface until saturation. In parts (a) and (c) the adsorption of molecules was randomly performed, while in parts (b) and (d) it was sequential. Figure 6a depicts the case where complex rotations are present and we see the formation of short double and simple chains. They are heterogeneous and dispersed. The variation of coverage is non-linear, see part (c). Figure 6b shows a sequential adsorption where complex and simple rotations are performed in the following sequence: $\alpha_3\uparrow\alpha_2\downarrow\alpha_3\downarrow\alpha_2\uparrow$. The non linear behavior of coverage is again present here. This is directly related to the fact that the volume excluded by α_3 is greater that the one excluded by α_2, i.e., it is easier to adsorb the second than the first one. Besides, the better assembly (both steric and energetically) is the one joining $\alpha_3\uparrow\alpha_3\downarrow$ or $\alpha_3\uparrow\alpha_2\downarrow$ (conversely, $\alpha_3\downarrow\alpha_3\uparrow$ or $\alpha_3\downarrow\alpha_2\uparrow$). When the adsorption mechanism is such that rotations are allowed, the pairs $\alpha_3\uparrow\alpha_3\downarrow$ or $\alpha_3\uparrow\alpha_2\downarrow$ are the most favorable. But, as we will see below, if the promotion of sites is also present, those pairs conform long and organized

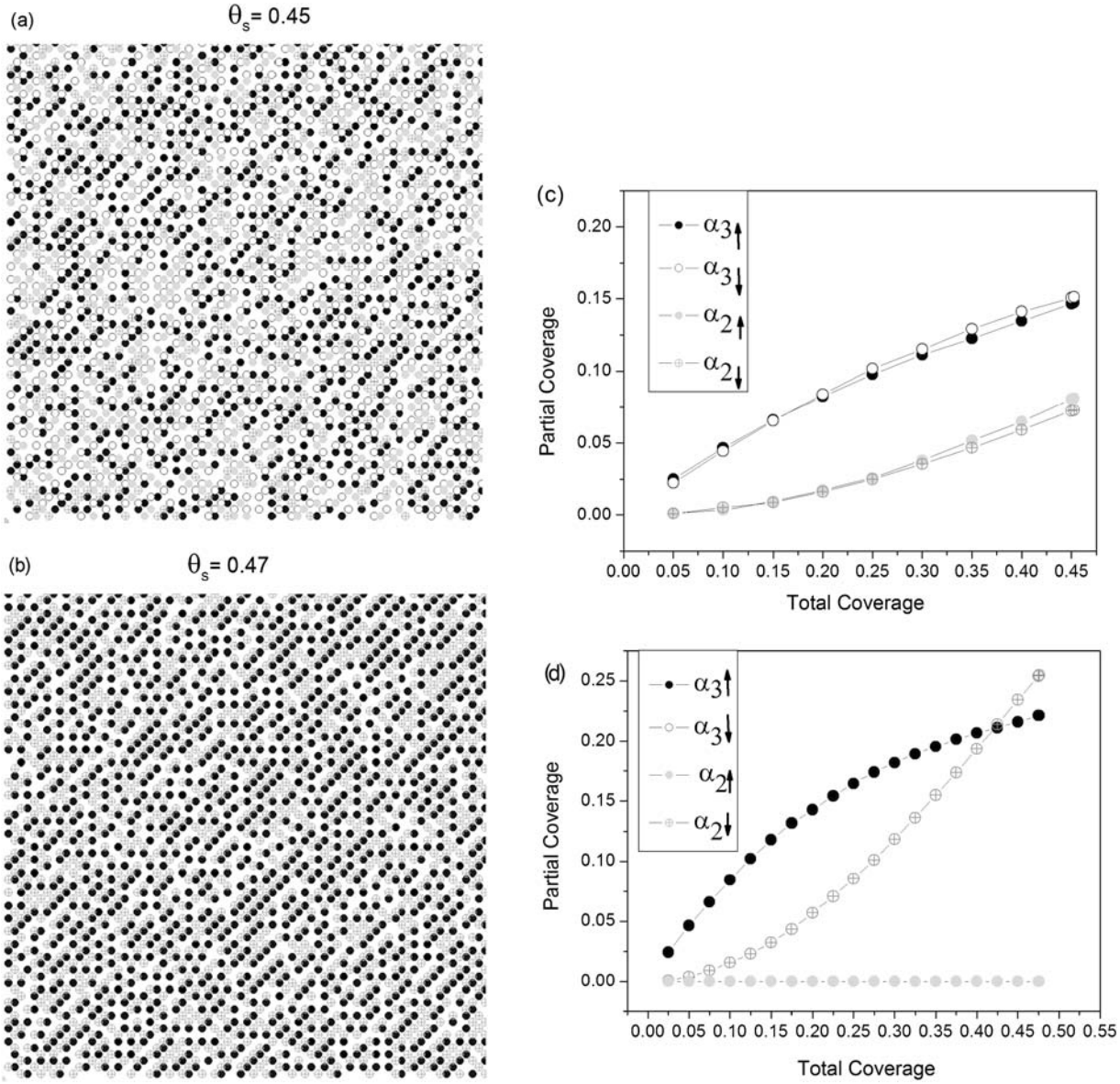

Fig. 6 Snapshots of surfaces belonging to the first group of model B. (**a**) Rotations are allowed with a random adsorption mechanism without promotion. (**b**) Rotations are allowed with a sequential adsorption mechanism ($\alpha_3\uparrow\alpha_2\downarrow\alpha_3\downarrow\alpha_2\uparrow$) without promotion. The symbols here are the same as those indicated in parts (**c**) and (**d**). These last parts show the coverage for each species against the total coverage of the surface until saturation for parts (**a**) and (**b**), respectively

chains that efficiently fill the surface and no steric effects appear. The absence of strong adsorbate-substrate interactions, simulated by a non-promoting mechanism, causes random adsorption to be less efficient and steric effects show up.

The main difference between Figs. 6a and 6b is that adsorption is random in the first, giving the same likelihood to species $\alpha_3\uparrow$ and $\alpha_3\downarrow$, thus both species $\alpha_2\uparrow$ and $\alpha_2\downarrow$ can compete for occupation of the non-inhibited sites on the surface. On the other hand, the mechanism employed in part (b) is sequential, favoring, in first place, the adsorption of $\alpha_3\uparrow$ and then of $\alpha_2\downarrow$; the other species being in the last steps of the sequence and, for that reason, their likelihood of being adsorbed is almost null.

Long range order We begin the simulation using an initial coverage of random adsorbed molecules with a defined footprint (α_3), representing the initial adsorption on defects of the substrate. The richness of the patterns is due to the different adsorption mechanisms employed (random or sequential) and to the fact that molecules can rotate before they adsorb (simple or complex rotations). We find the development of long double and single chains of molecules with different topological features. There are condensed phases

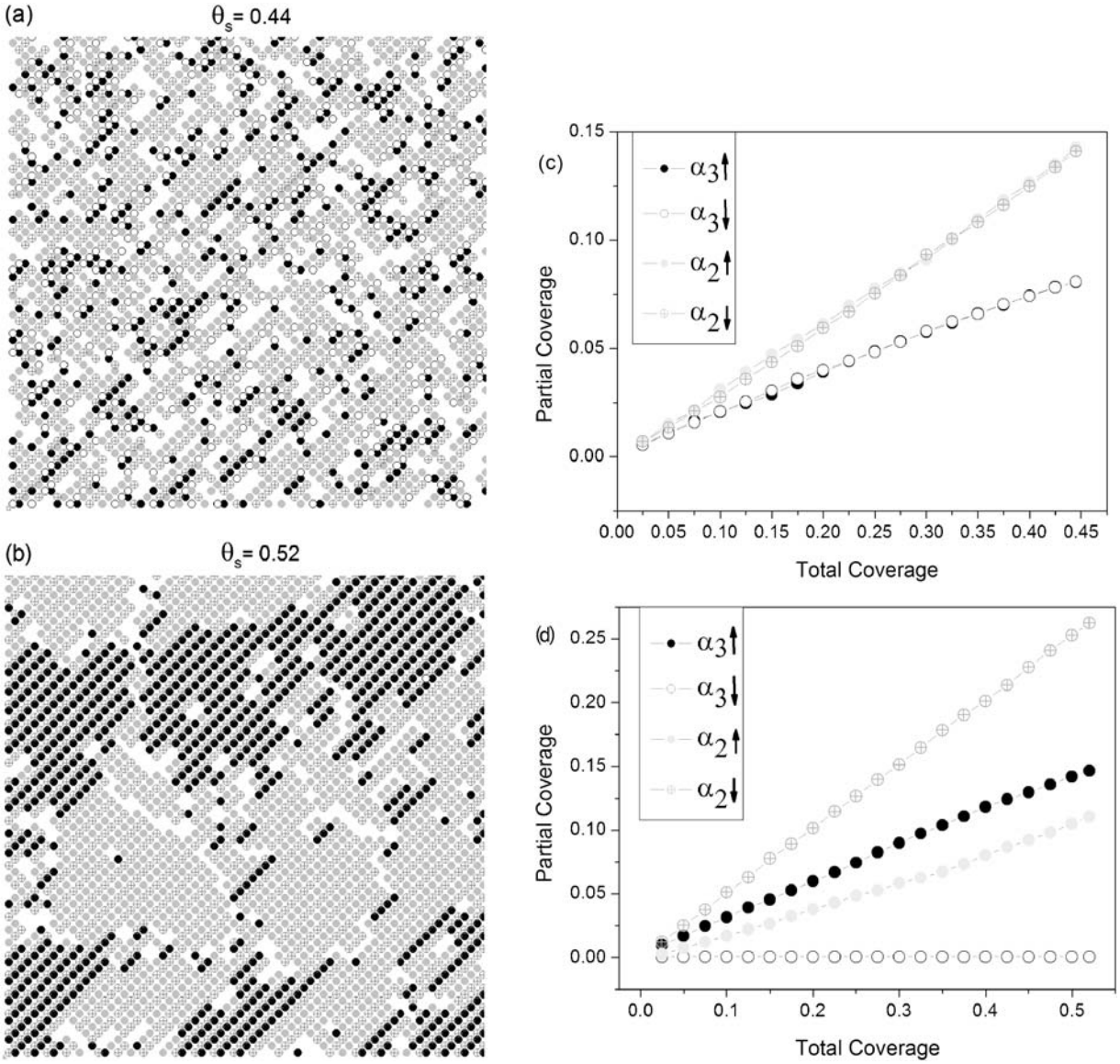

Fig. 7 Snapshots of surfaces belonging to the second group of model B, with their respective coverage for each species against the total coverage of the surface until saturation. (**a**) Rotations are allowed with a random adsorption mechanism with promotion. (**b**) Sequential adsorption with promotion. Sequence: $\alpha_3\uparrow\alpha_2\downarrow\alpha_3\downarrow\alpha_2\uparrow$. The symbols here are the same as those indicated in parts (**c**) and (**d**) where the respective coverage is shown as a function of total coverage

related to the promotion of neighboring sites when a molecule is added on the surface, favoring the adsorption of new ones.

Figure 7 shows two examples belonging to this group. Here again, the upper part of the figure is a snapshot of the adsorbed molecules on the substrate and the lower part gives the behavior of the coverage for each species against the total coverage of the surface until saturation. They were generated with a mechanism of promotion of sites for adsorption, i.e., molecules can only adsorb on promoted sites of the network and each time a new molecule is added to the surface their neighboring sites (gray sites) are promoted for new molecules. This strong molecule-substrate interaction causes the formation of clusters of different sizes formed by long chains along the preferential direction.

In what follows, we present an example for a random mechanism, Fig. 7a, and for a sequential one, Fig. 7b. Further examples of other different sequences in the order of adsorption of footprints are depicted and discussed elsewhere (Uñac et al. 2007).

In Fig. 7a we show a surface for random adsorption with rotations, like in Fig. 6a, but here with promotion of sites. We can see two main features. First, α_2 adsorption is greater than the one obtained when rotations are not allowed (Uñac

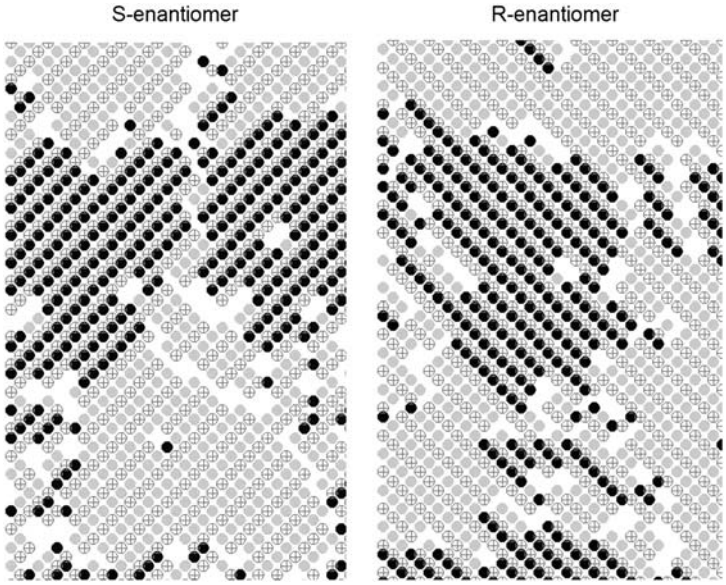

Fig. 8 Two mirror snapshots for the case of adsorption already depicted above in Fig. 7(b). The *left part* of the figure shows adsorption of S-enantiomers and the *right one* corresponds to R-enantiomers. Symbols are the same as in Fig. 7b

et al. 2007), and second, simple alternated $\alpha_2\uparrow\alpha_2\downarrow$ chains show up, forming more irregular shaped clusters. Due to the fact that the molecule can have complex rotation, it occupies sites that do not favor the later adsorption of α_3 species, thus, no pairs $\alpha_3\uparrow\alpha_3\downarrow$ are formed. This will increases the final total coverage, θ_S, compared to the one that would be obtained if no rotations were allowed (Uñac et al. 2007). Comparing Figs. 7a and 6a, we also find a greater adsorption of α_2 due to promotion effects; see Fig. 7c.

Finally, in Fig. 7b, where the sequence $\alpha_3\uparrow\alpha_2\downarrow\alpha_3\downarrow\alpha_2\uparrow$ is used, we observe, the strong trend of species $\uparrow\downarrow$ to form a compact pair (steric effect) that occupies most efficiently the surface, giving place to the growth of large chains condensed in big clusters. The formation of two well defined domains is present. These domains are single chains of α_2 species and double chains of $\alpha_3\uparrow\alpha_2\downarrow$ species, the last one minimizing excluded surface effects.

It is worth to mention that in this long range order group, the partial coverage of each of the adsorbed species increases always linearly with the total coverage, as seen in the lower part of Fig. 7. No competition among the different species is expected due to the mechanisms of adsorption employed in this group.

In all the above cases the biased direction of the chains on the surface is unique and it is definitely associated with the chiral character of S-molecules, independently of any adsorption feature.

3.1.3 Racemic mixture

For model B, the same cases developed above were repeated for pure R-molecules adsorption. All the features found reproduce the same results like those for S-molecules but here the patterns resulted to be the mirror image of the previous ones, i.e., the only difference noted was the change in the direction of the chains on the surface. This fact is in coincidence with the behavior found experimentally (Barlow and Raval 2003; Barlow et al. 2005). In Fig. 8 we show two mirror snapshots for the case of adsorption already depicted above in Fig. 7b. The left part of the figure shows adsorption of S-enantiomers and the right one corresponds to R-enantiomers. As clearly seen, adsorption of R-enantiomers confirms that the chiral growth direction of the chains is directly controlled by the local chirality of the adsorbed mole-

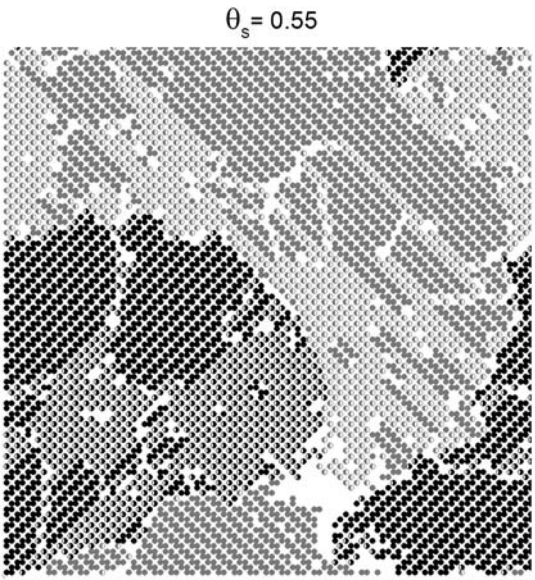

Fig. 9 Example of a typical surface obtained for a racemic adlayer, i.e., R and S enantiomers are adsorbed with the same probability. Here we use a sequential adsorption process. Symbols represent: *solid black circle* (S-$\alpha_3\uparrow$, S-$\alpha_3\downarrow$); *semi-solid black circle* (S-$\alpha_2\uparrow$, S-$\alpha_2\downarrow$); *solid gray circle* (R-$\alpha_3\uparrow$, R-$\alpha_3\downarrow$); *semi-solid gray circle* (R-$\alpha_2\uparrow$, R-$\alpha_2\downarrow$)

cules. The chains now grow parallel to the mirror direction of S-chains, as illustrated by the figure.

In this way, our simulations confirm the statement already expressed in experimental works (Barlow and Raval 2003; Barlow et al. 2005): the chiral character of molecules is directly transferred to the metallic surface. For this reason and for the sake of briefness, we do not show here results for adsorption of pure R-enantiomers. Nevertheless, to illustrate the behavior of a racemic mixture of S and R enantiomers, we show one case in Fig. 9, where clearly different domains of S and R clusters with their pertinent directions are shown with quite good agreement with experiments (Barlow and Raval 2003; Toomes et al. 2003; Barlow et al. 1998, 2004).

4 Conclusion

The main results found here resemble qualitatively some of the features shown and discussed in experiments by many authors (Barlow and Raval 2003; Stensgaard 2003; Chen et al. 2002; Toomes et al. 2003; Barlow et al. 1998, 2004, 2005).

In the context of model A, we have tried some of the footprints (chiral motifs) proposed by others (Barlow and Raval 2003) showing that, within the assumptions made here, one cannot get condensed phases although interactions such as adsorbate-substrate and adsorbate-adsorbate are taken into account, as, for example, in Fig. 3, case 1, where double chains of molecules $\alpha_3\alpha_2$ are developed giving rise to very large and twin chain structures. There is a markedly tilted alignment of the chains. No compact phases appear. However, in case 2 we observe that the footprint used for α_3 species is better assembled on the surface, growing in an ordered array oriented in a tilted preferential direction. It is worthy to point out here that the election of the chiral center for the adsorption motif is directly related to the efficiency with which molecules accommodate on the surface. See Figs. 3a and Fig. 4a.

On the other hand, the presence of the tilted α_2 motif, as in case 4, is crucial for the appearance of two different orientations on the surface. This shows up clearly when comparing Figs. 3b and Fig. 4a.

Finally in this model, the mixture of two triangular footprints simultaneously produced two different condensed phases. Inside each phase, we find molecules with only one type of adsorption motif. They form single chains with two different preferential directions, one for each phases, this last result has not been observed experimentally to our knowledge. Besides, the steric effects prevent the growth of double chains. See Fig. 5.

In general, given the results using this simple model and according to the experiments in Barlow et al. (2005), we conclude that a chiral molecule, like for instance alanine, transfers its chiral character to its footprint as a unique motif (with a given and definite orientation in the surface) in such a way that a molecule with a given chirality can not give rise to different chiral footprints. Otherwise, in experiments it would be found the existence of chains following more than one overall growth direction.

Regarding model B, the steric effect observed in the first group resembles the behavior of systems such as alaninate on Cu(110) (Barlow et al. 2004, 2005). Besides, this model can generate many patterns using very simple rules and can be compared with those used in Mao et al. (2002).

In our results, it is evident that the chiral character of the adsorbate is transferred to the substrate. The two main behaviors: long and short range chains assemblies, are related, respectively, to the promotion and non promotion of sites and the steric effects present in the model. From the results of the racemic mixture, the development of chiral domains on the surface is clear and explains the patterns obtained experimentally (Barlow et al. 2005; Humblot and Raval 2005; Raval 2003).

Finally, these simple models provide a basis for the understanding of the behavior of complex adsorption systems in which chiral molecules interact with a metallic surface.

Acknowledgements This work was supported by the Agencia Nacional de Investigaciones Científicas y Técnicas of Argentina. Thanks are also due to CONICET.

References

Barlow, S.M., Raval, R.: Surf. Sci. Rep. **50**, 201 (2003)
Barlow, S.M., Kitching, K.J., Haq, S., Richardson, N.V.: Surf. Sci. **401**, 322–335 (1998)
Barlow, S.M., Louafi, S., Le Roux, D., Williams, J., Muryn, C., Haq, S., Raval, R.: Langmuir **20**, 7171 (2004)
Barlow, S.M., Louafi, S., Le Roux, D., Williams, J., Muryn, C., Haq, S., Raval, R.: Surf. Sci. **590**, 243 (2005)
Chen, Q., Frankel, D.J., Richardson, N.V.: Surf. Sci. **497**, 37–46 (2002)
Humblot, V., Raval, R.: Appl. Surf. Sci. **241**, 150 (2005)
Humblot, V., Barlow, S.M., Raval, R.: Progr. Surf. Sci. **76**, 1 (2004)
Mao, L., Harris, H.H., Stine, K.J.: J. Chem. Inf. Comput. Sci. **42**, 1179 (2002)
Ranking, R.B., Sholl, D.S.: Surf. Sci. **548**, 301 (2004)
Ranking, R.B., Sholl, D.S.: Surf. Sci. **574**, L1 (2005)
Raval, R.: Current Opinion Sol. State Mater. Sci. **7**, 67 (2003)
Romá, F., Stacciola, D., Tysoe, W.T., Zgrablich, G.: Physica A **338**, 493 (2004)
Stensgaard, I.: Surf. Sci. **545**, L747 (2003)
Toomes, R.L., Kang, J.-H., Woodruff, D.P., Polcik, M., Kittel, M., Hoeft, J.-T.: Surf. Sci. **522**, L9–L14 (2003)
Uñac, R.O., Gil Rabaza, A.V., Vidales, A.M., Zgrablich, G.: Appl. Surf. Sci. **254**, 7795 (2007)
Williams, J., Haq, S., Raval, R.: Surf. Sci. **368**, 303 (1996)